


Article

Formulating Eco-Friendly Foamed Mortar by Incorporating Sawdust Ash as a Partial Cement Replacement

Samadar S. Majeed 

Civil Engineering Department, Nawroz University, Duhok 42001, Iraq; samadar.salim@nawroz.edu.krd;
Tel.: +964-750-459-4636

Abstract: Utilizing sawdust efficiently to produce construction materials can help safeguard the environment and decrease costs by minimizing the need for traditional resources and reducing carbon dioxide (CO₂) emissions. Additionally, recycling sawdust plays an essential role in creating a sustainable ecosystem. Hence, this study aimed to examine the potential use of sawdust ash (SDA) as a partial cement replacement on foamed mortar (FM) properties, including its fresh, mechanical, transport, thermal, and microstructural properties. A variety of FM mixtures were tested for workability, density, consistency, intrinsic air permeability, porosity, split tensile strength, compressive strength, flexural strength, and thermal conductivity by replacing cement with SDA at varying percentages of 0%, 10%, 20%, 30%, 40%, and 50%. The results revealed that FM's workability was reduced by the introduction of SDA with a higher percentage cement replacement, while the density of the FM mixtures was reduced due to SDA's specific gravity being lower than that of cement. A linear improvement was observed in the air permeability, sorptivity, and porosity of FM–SDA composites with an increased SDA percentage to 20%. It is notable that these properties started to deteriorate once the cement replacement by SDA surpassed 30%. A noticeable improvement of mechanical strength properties of the FM was found at 20% of SDA content, but they deteriorated when the SDA content was more than 30%. FM blends with higher SDA contents exhibited larger and more apparent voids, according to SEM analysis. In conclusion, incorporating sawdust into formulations emerges as a viable method for FM production. This approach not only mitigates the environmental impact of sawdust disposal but also reduces the need for extracting natural resources in construction material manufacturing.



Citation: Majeed, S.S. Formulating Eco-Friendly Foamed Mortar by Incorporating Sawdust Ash as a Partial Cement Replacement. *Sustainability* **2024**, *16*, 2612. <https://doi.org/10.3390/su16072612>

Academic Editors: Sathees Nava,
Sayanthan Ramakrishnan
and Kirubajiny Pasupathy

Received: 19 February 2024

Revised: 11 March 2024

Accepted: 19 March 2024

Published: 22 March 2024



Copyright: © 2024 by the author. Licensee MDPI, Basel, Switzerland. This article is an open access article distributed under the terms and conditions of the Creative Commons Attribution (CC BY) license (<https://creativecommons.org/licenses/by/4.0/>).

Keywords: foamed mortar; sawdust ash; green material; sustainable concrete; compressive strength; thermal conductivity; permeability

1. Introduction

The concept of foamed mortar (FM) is widely understood to be a flexible and lightweight material that possesses a consistently dispersed pore structure, which is obtained through the mechanical injection of air in the form of tiny bubbles [1–5]. The composition of this material consists of Portland cement paste or a cement filler matrix (mortar), with a minimum total volume of 20% [6]. The density of FM can be adjusted within the range of 400 to 1600 kg/m³ [7]. It possesses various appealing attributes, including effective thermal and acoustic insulation, ease of manufacturing, and self-flowing properties [8–10]. Nevertheless, FM has low mechanical qualities in comparison to regular concrete. Consequently, it would be more advantageous to employ FM in the building of low-rise dwellings as a partition or load-bearing wall [11].

Foamed mortar provides unique attributes such as decreased density, the ability to self-level, cost-efficiency, low thermal conductivity, and notable fire resistance [12–16]. These characteristics make it appropriate for various applications, including filler materials, insulation materials, and foundational building materials with limited load-bearing capacity. Implementing FM has the capacity to significantly decrease the total weight of

a building, hence potentially reducing the risk of damage caused by earthquakes [17–20]. Furthermore, the implementation of FM significantly reduced the consumption of cement and aggregate materials [21,22]. It has been noted that the cement production process contributes to around 6% of the total global carbon dioxide (CO₂) emissions. This might be due to the occurrence of diverse chemical emissions across all phases of this industry. Consequently, it is widely acknowledged that a significant proportion of environmental pollution on a global scale may be attributed to the utilization of these materials [23].

Nambiar and Ramamurthy [24] employed two distinct approaches to incorporate pores inside FM. The first way involved the formation of foam prior to its addition to the mixture, while the second method entailed the incorporation of a foaming agent. Furthermore, FM used in this study was generated by foaming using the prepared technique. The pore structure of cementitious materials has a pivotal role in determining significant qualities, including strength and durability. The porosity and permeability of the material were contingent upon the configuration of its pores. However, it is insufficient to solely ascertain the overall air void content of a substance, commonly referred to as its porosity. The strength and durability of concrete are influenced by the shape, size, and distribution of these voids [25,26]. A study conducted by Jalal et al. [27] provided evidence supporting the suitability of FM as a construction material in industrialized building systems due to their adequate strength. The material can be employed to effectively occupy empty spaces and gaps across extensive distances within a construction endeavor, without necessitating supplementary vibration or compaction.

Kearsley and Wainwright [28] suggested that the compressive strength of FM, as determined by tests conducted at 28-day and 1-year intervals, was predominantly influenced by dry density, and stayed unaltered by the proportion of cement substituted with ash. Moreover, the researchers demonstrated that augmenting the substitution of cement with fly ash did not have a substantial impact on the compressive strength of the fly ash, provided there was an effective curing process. Furthermore, it has been observed that the strength of concrete can be enhanced through the reduction of sand particle size [29,30]. The manufacturing of FM requires the use of cement, which, like other cement-based concretes, has a harmful effect on the natural environment. Furthermore, the cement industry is associated with the phenomenon of global warming, mostly because of the production of substantial quantities of carbon dioxide. These emissions have a direct impact on climate change and contribute to environmental degradation. Prior studies have demonstrated that the cement industry accounts for approximately 8% of global industrial emissions [31,32].

The accumulation and utilization of sawdust in concrete have emerged as a significant issue in the construction industry. Sawdust, a byproduct of timber processing, poses several challenges in terms of disposal and environmental impact [33]. With the increasing demand for sustainable building materials, finding ways to incorporate sawdust in concrete production has become a priority. Although sawdust can enhance thermal insulation and reduce the weight of concrete, its inclusion can compromise the strength and durability of the material. To address this problem effectively, researchers have been investigating various methods to treat sawdust before incorporating it into concrete mixes. These treatments aim to mitigate the negative effects of sawdust on the structural properties of concrete while maximizing its beneficial attributes. By striking a balance between sustainability and performance, the industry can leverage the potential of sawdust as a valuable resource in concrete production.

Thermal modification of sawdust involves treating sawdust at high temperatures to dry it and remove volatile compounds. This results in a more stable, durable material that can then be used as a partial replacement for standard aggregates in concrete. The sawdust treated with either hot water or with boiling alkali-added water has a positive effect on the performance of Wood-Crete according to Aigbomian and Fan [34]. The compressive strength can be increased by about 30% and 260% for hot water boiling treatment and hot water with 4% sodium hydroxide (NaOH) treatment, respectively.

The wood industry is widely recognized for producing a substantial quantity of trash, commonly known as sawdust. An effective approach to addressing this waste is to employ wood as a primary resource for energy production. However, a new issue has arisen due to the thermal combustion process, which reduces both the bulk and volume of the wood waste, yet results in the production of wood ash, also known as sawdust ash. Incineration, the traditional method for managing sawdust, releases toxic and hazardous gases and pollutants into the environment. To address this problem, various uses have been developed for sawdust, including its use as a fuel source in thermal processes, its application as an insulating and construction material, its incorporation as woody biomass in compost production, and its effectiveness as an adsorbent in removing contaminants such as dyes, heavy metals, pharmaceutical products, and emerging pollutants. The characteristics of the produced sawdust are primarily determined by the types of wood and the diameters of the saw teeth. The particles can be categorized into three groups according to their size: oversized particles (OS) for particles larger than 710 μm , coarse particle size (CPS) for particles between 24 and 60 mesh (350–710 μm), and fine particle size (FPS) for particles between 60 and 80 mesh (177–350 μm) [35–37]. The present investigation employed sawdust samples characterized by the following particle size and grain composition: 80.1% of the samples passed a diameter of 45 μm , the median particle size was 19.5 μm , and the maximum particle size was 75.5 μm . The sawdust underwent incineration until it reached a size that allowed it to pass through a 45 μm (No. 325) filter. Based on the ASTM criteria, it was categorized as a member of the Class F group of pozzolans. In addition, the sawdust was acquired from commercial sawmills located in Penang, Malaysia, and thereafter stored under ambient humidity conditions at room temperature.

The disposal of sawdust in exposed locations can result in adverse health effects for humans, as shown in Iraq and other developing nations. This is due to the incineration of these waste materials, which contributes to pollution and other environmental issues. Hence, the application of sawdust continues to provide challenges and poses potential risks to the ecological and environmental systems. Wood sawdust ash was utilized as a pozzolan in concrete as a partial substitute for cement or aggregate in recent experiments [18–21]. The ideal range for the compressive strength of cement mixed with wood ash, as determined by Sajjad et al. [38], was found to be between 10% and 20% by weight of the binder. In a study conducted by Abdullahi et al. [39], sand was substituted with sawdust at different proportions, ranging from 10% to 50%. The research entailed the fabrication of cubes of conventional dimensions (150 mm) to ascertain the compressive strength of the concrete. The best dosage, as determined by the British Standard (BS) code, was found to be 10%, as it was within the prescribed range and strength level outlined by the code. Nevertheless, the investigation determined that due to its propensity to induce fluctuations and reductions in strength, the concrete was unsuitable for structural applications. Bikila et al. [40] employed dosages of up to 100%, with increments of 25%, in a comparable endeavor to partially substitute sand. The sand's homogeneity and curvature coefficients were measured to be 1.049 and 1.324, respectively. These values demonstrate that the material meets the appropriate grade and quality standards set by British Standards. Furthermore, the average crushing value of the sand satisfied the criteria outlined in the BS code. Nevertheless, the experimental findings indicated a negative correlation between the dosage of dust and the workability of the concrete. Moreover, the strength of concrete failed to fulfil the prescribed criteria for lightweight concrete when the dosage exceeded 25%. Hence, it was deduced that once the replacement exceeded 25%, the concrete exhibited a consistent trend of diminishing workability and strength.

Sawdust can be made through a variety of processes; in general, there are two methods. The first is the oxygen-based technique, where the sawdust is burned in the presence of oxygen to release heat and energy. This is typically performed in specialized incinerators or furnaces designed for burning biomass materials, like sawdust. The second is the oxygen-free technique, where sawdust is heated in a controlled environment with limited or no oxygen, so that it breaks down into biochar, bio-oil, and syngas without actually burning.

Narayanan et al. [41] conducted a study where they utilized sawdust as a partial replacement for sand in specified proportions to examine the density and strength of concrete. Additionally, it was observed that the sawdust exhibited a lower specific gravity of 0.27 and a higher water absorption of 2 when compared to ordinary sand. The researchers additionally observed a drop in the density and strength of M20 grade concrete (with a water-to-cement ratio of 0.5) with an increase in the quantity of sawdust. Therefore, it was determined that sawdust has the potential to be employed in both conventional and lightweight non-structural components. Velmurugan and Jose [42] reached a comparable finding regarding the mortar block, workability, and compressive strength of M30 grade concrete by laboratory-based tests of concrete density. Moreover, the authors contended that the utilization of trash not only exhibits environmentally sustainable practices but also yields economic advantages. Moreover, existing literature has established that it exerts a beneficial impact on the advancement of lightweight concrete, exhibiting an ideal dose of up to 20%. This study primarily aims to examine and analyze the fresh-state properties, mechanical characteristics, behaviors at elevated temperatures, microstructure, and transport properties of foamed mortar that incorporate varying percentages of sawdust range (10%, 20%, 30%, 40%, and 50%) as a partial replacement for cement, based on a comprehensive review of previous research.

Novelty and Research Significance

There has been a lack of studies conducted to evaluate the effects of SDA on the several properties of FM, including fresh-state, mechanical, thermal, and transport properties. Although there are limitations on the accessibility of commercially processed sawdust for use in FM, it is regarded as one of the most favorable forms of SDA for this specific use. The integration of SDA into cementitious materials has been the subject of limited investigation. Nevertheless, there are still several issues that remain regarding the underlying process through which SDA has the capacity to modify the characteristics of these materials. Moreover, the majority of the existing research has predominantly concentrated on normal-strength concrete. Thus far, there has been a dearth of scientific inquiries investigating the effects of SDA on facility management. The resolution of the uncertainty in this particular case is of utmost importance. Hence, it is imperative to examine the influence of SDA modification on the properties of both fresh and hardened concrete with respect to mechanical properties. A morphological investigation using a scanning electron microscope (SEM) was employed to validate enhanced mechanical capabilities.

2. Experimental Methods

2.1. Materials

The production process of the foamed mortar (FM) involved the utilization of four primary materials, specifically ordinary Portland cement (OPC), fine sand, a protein-based foaming agent, and potable water.

2.1.1. Ordinary Portland Cement

In accordance with the requirements of CEM 1; BS197-1 [43], the cement selected was mostly adherent to Portland cement international standards, and it was provided locally. Table 1 presents the cement's physical properties.

Table 1. Chemical composition of the cement used in this investigation.

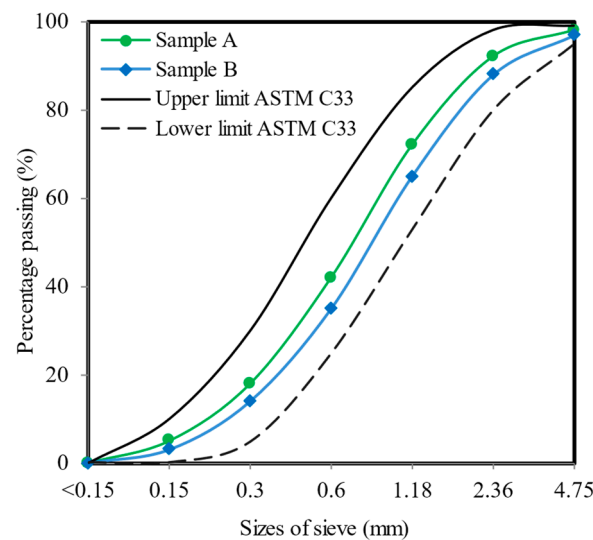
Elements	Percentage (%)
Calcium oxide (Cao)	66.97
Silicon dioxide (SiO ₂)	13.99
Iron oxide (Fe ₂ O ₃)	7.57
Sodium oxide (Na ₂ O)	0.26
Magnesium oxide (MgO)	1.35

Table 1. *Cont.*

Elements	Percentage (%)
Aluminium oxide (Al_2O_3)	4.01
Potassium oxide (K_2O)	0.90
Sulfur trioxide (SO_3)	4.95

2.1.2. Fine River Sand

Fine river sand was used as the sand for this study; its major properties were a specific gravity of 2.55 and a saturated surface dry specific gravity of 2.60. In addition, the grading of the river sand utilized in the present work (Figure 1) was compliant with ASTM C33-03 [44].

**Figure 1.** Sand grading curve.

2.1.3. Water

The mix was prepared using potable water. The water used was adherent to the standards of BS-3148 [45].

2.1.4. Foaming Agent

A protein-based foaming agent known as Norait PA-1, supplied by DRN Technologies Sdn Bhd, Kuala Lumpur, Malaysia, was utilized as a surfactant to produce stable foam in the mortar slurry. This foaming agent can create foam with the ability to reach a density of 80 kg/m^3 when mixed with water at a 1:30 ratio. Table 2 provides the properties of this facility.

Table 2. Foaming agent properties.

Properties	Descriptions/Values
Color	Dark brown
Type	Protein-based
Foam density (kg/m^3)	70–80
Specific gravity	1.20
Acidity (pH)	6.35–6.45
Boiling point ($^{\circ}\text{C}$)	130
Vapor pressure (kPa)	40
Expansion proportion	25–35 ×
Viscosity (cps)	590

2.1.5. Sawdust

Sawdust ash (SDA) was employed as partial cement replacement in the production of FM. Raw sawdust was supplied by BE Green Biomass Sdn. Bhd., Malaysia. The raw sawdust was sieved to eliminate any unwanted residue. Figure 2 shows the sawdust employed in this study. Table 3 compares the physical properties of sawdust, OPC, and sand. The sawdust percentages used for the cement replacement were 10%, 20%, 30%, 40%, and 50%, along with the control mix. Table 4 shows the chemical composition of sawdust employed in this study.

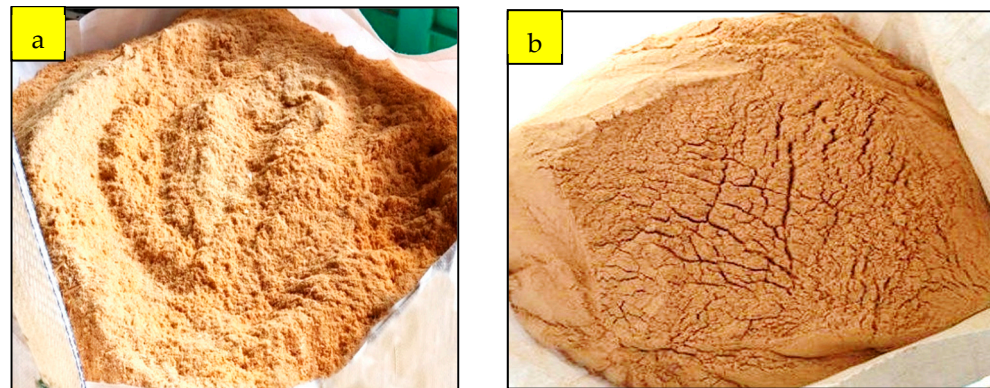


Figure 2. Sawdust used in this study: (a) raw sawdust; (b) sieved sawdust ash (SDA).

Table 3. Physical properties of sawdust, OPC, and sand.

Component	Cement	Sand	Sawdust
Bulk density (kg/m^3)	1430	1680	690
Moisture absorption (%)	2.75	2.14	2.02
Fineness modulus	-	2.29	2.45
Specific gravity	3.15	2.55	2.06
Specific surface area (m^2/kg)	365	458	672
Bulk porosity (%)	-	29.5	28.0

Table 4. Foamed mortar mix designs.

Mix Ref.	Designed Density (kg/m^3)	Sawdust (%)	Sawdust (kg/m^3)	Cement (kg/m^3)	Sand (kg/m^3)	Water (kg/m^3)	Foam (kg/m^3)
SDA0	850	0	0.00	270.10	540.3	135.1	35.3
SDA10	850	10	27.01	243.09	540.3	135.1	35.3
SDA20	850	20	54.02	216.08	540.3	135.1	35.3
SDA30	850	30	81.03	189.07	540.3	135.1	35.3
SDA40	850	40	108.04	162.06	540.3	135.1	35.3
SDA50	850	50	135.05	135.05	540.3	135.1	35.3

2.2. Mix Proportions

A total of six foamed mortar (FM) mixtures were prepared. The mixture compositions of the FM with varying percentages of sawdust cement replacement are displayed in Table 4. The control mix consists of 0% sawdust cement replacement, whereas the remaining mixtures consist of 10%, 20%, 30%, 40%, and 50% sawdust cement replacement. The FM exhibited the highest level of workability when the water-to-cement ratio was 0.5, but the ideal cement-to-sand ratio was determined to be 1:2. Furthermore, an FM with a low density of $850 \text{ kg}/\text{m}^3$ was manufactured and subjected to testing. The FM mix designs with different weight fractions of sawdust are presented in Table 3. The manufacturing of

the FM involved the utilization of four primary materials: ordinary Portland cement (OPC), fine sand, a protein-based foaming ingredient, and potable water.

2.3. Experimental Setup

2.3.1. Sawdust Characterizations

In order to analyze the characteristics of the sawdust utilized in the present study, scanning electron microscopy (SEM) evaluation, X-ray diffraction (XRD) analysis, and X-ray fluorescence spectroscopy (XRF) were performed. The SEM was performed using an Olympus VS200 instrument. The Bruker XRD D8 Advance instrument was utilized to determine the XRD of the SDA specimen. In order to ascertain the chemical contents of sawdust, XRF was employed.

2.3.2. Fresh-State Properties

The flow table test was employed to assess the workability of the foamed mortar and ascertain the moisture transportability limit. Crucial procedures for carrying out the test involved cleansing and eliminating any contaminants, such as dust or concrete, that remained from prior testing on the surface where the concrete was to be placed, to avoid any disruption to the outcomes. A flow table test was conducted on recently mixed concrete, adhering to the specifications outlined in ASTM C 230-97 [46]. The values of the flow table were obtained by the utilization of the static free-flow test method, wherein the material undergoes flow solely under the influence of static gravity, as depicted in Figure 3a. Furthermore, the consistency was determined by calculating the setting time, following the guidelines established in BS EN 196-3 [47]. The measurement was conducted using the Vicat apparatus, as depicted in Figure 3b, and was expressed in grams. Furthermore, the density of the newly mixed concrete was determined using the BS 12350-6 [48] standard, as depicted in Figure 3c.

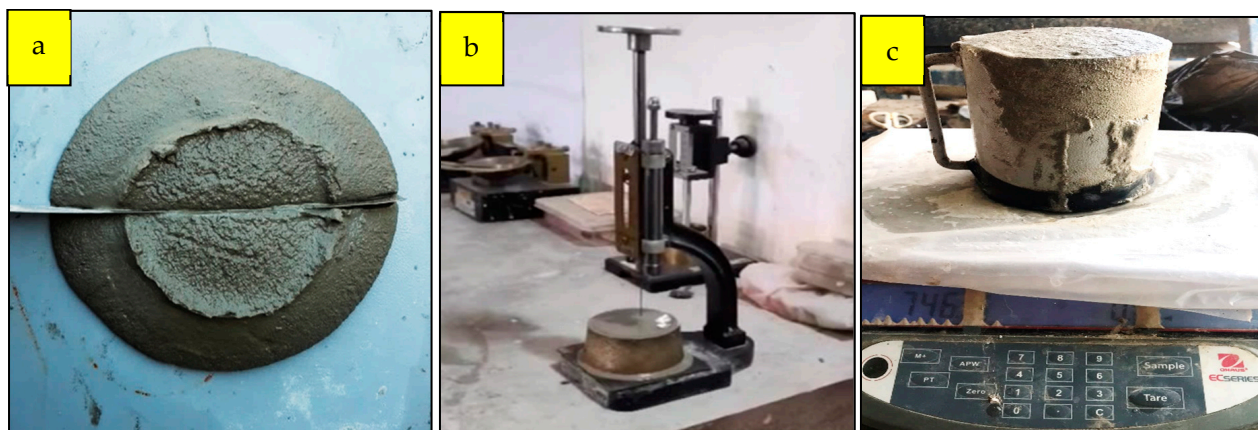


Figure 3. Set up for fresh-state tests. (a) Flow table test. (b) Consistency test. (c) Fresh density measurement.

2.3.3. Transport Properties

In order to ascertain the intrinsic air permeability, cylindrical samples measuring $55 \text{ } \phi \times 50 \text{ mm}$ were utilized following a 28-day curing period. The methodology proposed by Cabrera and Lynsdale [49] was employed, as depicted in Figure 4a. The porosity of the FM mixes was assessed using vacuum saturation equipment. Cylindrical samples measuring $75 \times 100 \text{ mm}$ were tested after 7, 14, 28, and 90 days of curing, using the methodology outlined by Cabrera and Lynsdale [35]. The results are illustrated in Figure 4b. The porosity was determined by employing Equation (1) [49]:

$$P = \frac{(W_{sat} - W_{dry})}{(W_{sat} - W_{wat})} 100 \quad (1)$$

where P is the vacuum saturation porosity (%), W_{sat} is the weight of the saturated sample in air, W_{wat} is the weight of the saturated sample in water, and W_{dry} is the weight of the oven-dried sample.

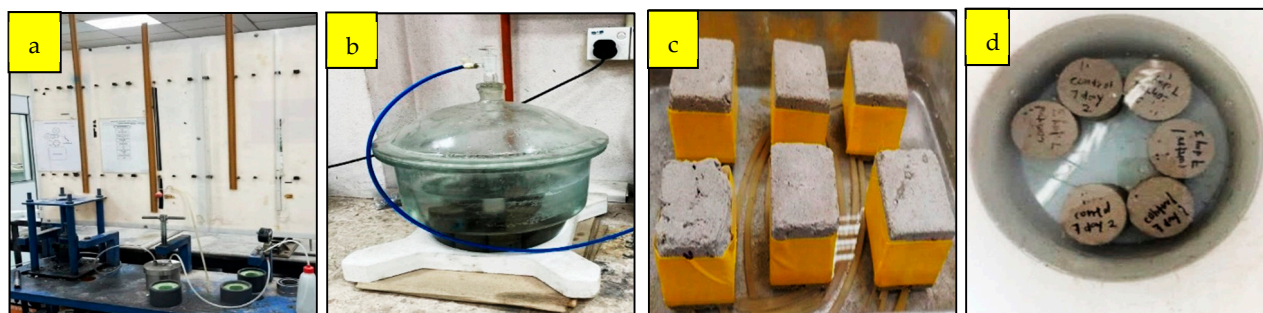


Figure 4. Set up for permeability tests. (a) Intrinsic air permeability test. (b) Porosity test. (c) Water absorption test. (d) Sorptivity test.

FM absorption properties were determined using the sorptivity test, which measured the rate of water absorption through the pores of the concrete via capillary action. The specimens were dried in an oven preheated to 100 ± 5 °C until their mass remained constant. Subsequently, the experiment was conducted. To inhibit water absorption by the sides of the cube sample ($50 \times 50 \times 50$ mm), paraffin was applied to all surfaces of the specimen. The experiment was conducted on the concrete surface area that was in direct contact with water, as illustrated in Figure 4c. Subsequently, the FM specimens were extracted from the container and assessed for mass gain at various time intervals (10, 20, 30, 40, 50, and 60 min) by weighing them. We computed the volume of water ingested by dividing the mass gained by the nominal surface area of the specimen and by the density of water. Subsequently, the slope of the line representing the relationship between time and these values was utilized to calculate the sorptivity coefficient (index) of the concretes, as specified in ASTM C1403-15 [50]. To assess the water absorption characteristics of the FM, three-cylinder cores measuring $75 \varnothing \times 100$ mm were fabricated and subjected to testing in accordance with the curing schedule on days 7, 14, 28, and 90 [51]. The experimental setup is illustrated in Figure 4d.

2.3.4. Mechanical Properties

Various experiments were performed to determine the mechanical properties of FM, encompassing compressive strength, flexural strength, splitting tensile strength, and Young's modulus. The compressive strength tests were conducted using FM cubes with dimensions of $100 \times 100 \times 100$ mm. These cubes were cured for varying durations (7, 14, and 28 days) and tested in accordance with the BS12390-3 standard [52], as shown in Figure 5a. The flexural tests were conducted using water-cured prism samples of $100 \times 100 \times 500$ mm after 7, 14, and 28 days. The tests followed the guidelines outlined in BS-EN 12390-5 [53], as shown in Figure 5b. Following that, as depicted in Figure 5c, cylinder specimens that had fully cured and had dimensions of 100×200 mm were inspected at 7, 14, and 28 days, following the guidelines outlined in BS12390-6 [54]. Figure 5d illustrates the Young's modulus test conducted on a sample cylinder of 100×200 mm after a curing period of 28 days, following the guidelines stated in ASTM C469 [55].

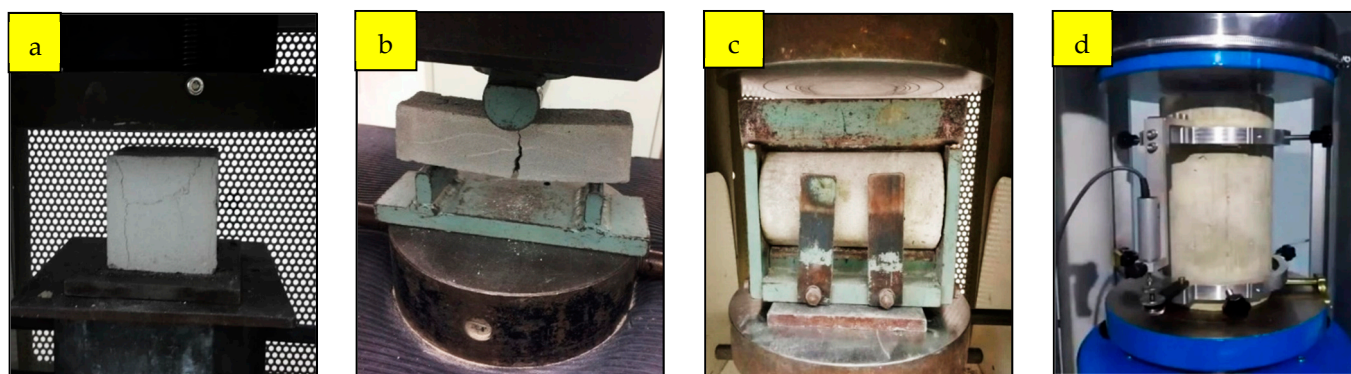


Figure 5. Setup for mechanical tests. (a) Compression test. (b) Flexural test. (c) Split tensile test. (d) Young's modulus test.

2.3.5. Thermal Conductivity Assessment

The thermal transmission properties of FM in a stable condition were determined through the application of the guarded hot plate (GHP) method. The analysis was performed on rectangular samples measuring $18 \times 18 \times 8$ mm, following a 28-day curing period. The experimental procedure followed the guidelines described in ASTM C177 [56], as it is shown in Figure 6.



Figure 6. Setup for thermal tests.

2.3.6. Microstructural Assessment

To ascertain the pore structure of the FM, a characterization analysis was performed using mercury intrusion porosimeter (MIP). This examination was carried out on rectangular samples that had been cured for 28 days and had dimensions of $15 \times 20 \times 5$ mm, using the methodology outlined in ASTM D4404-18 [57]. In addition, scanning electron microscopy (SEM) analysis was performed on samples measuring $12 \times 12 \times 12$ mm to investigate the impact of substituting cement with varying proportions of supplementary cementitious materials (SDA) on the pore distribution and volume. This is evident from the images obtained at a magnification of 120 after the samples have been cured in water for 28 days.

3. Results and Discussion

This section comprehensively presents the outcomes of our laboratory assessment of the effects of varying percentages of SDA cement replacement on the properties of FM. The properties assessed were workability, consistency, density, intrinsic air permeability, porosity, sorptivity, split tensile strength, compressive strength, flexural strength, and thermal conductivity.

3.1. Sawdust Characterization

The SEM was conducted using an Olympus VS200 device. Figure 7 visualizes the morphology of sawdust, while Figure 8 demonstrates the X-ray diffraction (XRD) pattern of the SDA. The X-ray diffraction of the SDA specimen was determined using a Bruker XRD D8 Advance device. The analysis of the XRD patterns indicated the presence of two prominent peaks at diffraction angles of 15.6° and 22.4° , which could be attributed to the (101) and (002) lattice planes of cellulose, respectively. At a diffraction angle of 34.7° , an additional minuscule peak was detected, which was ascribed to the (400) plane of crystalline cellulose. The presence of three distinct crystalline peaks at 2-theta angles of 16° , 24° , and 35° could be attributed to the crystallinity of the sawdust cellulose.

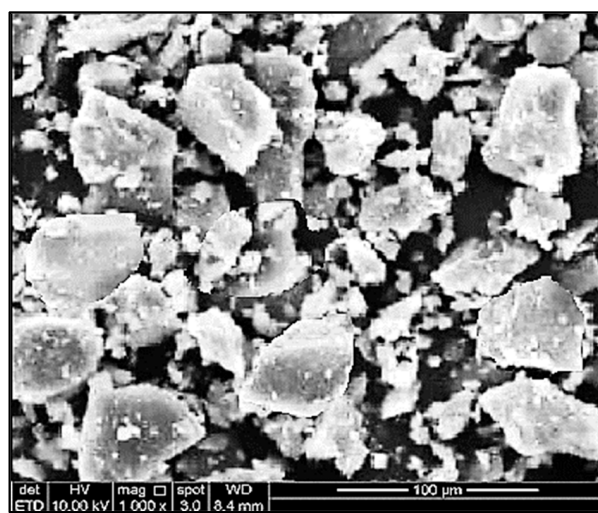


Figure 7. Sawdust morphology.

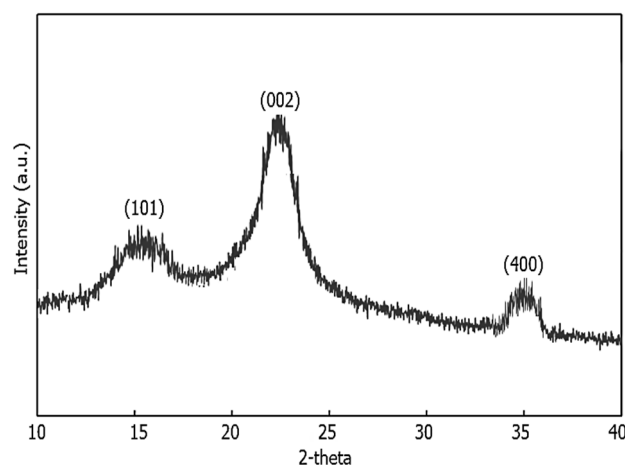


Figure 8. Sawdust XRD pattern.

The chemical composition of sawdust was determined using X-ray fluorescence spectroscopy (XRF), as shown in Table 5. The results shown in Table 5 demonstrate that sawdust predominantly consists of silicone dioxide, accounting for approximately 87% of its composition, in comparison to the other reactive substances. It is the main indicator of pozzolanic activity. Consequently, it can be employed as a substitute for conventional Portland cement in the production of foamed mortar.

Table 5. Chemical compositions of sawdust.

Component	Cement
Silicon dioxide	86.95
Aluminium oxide	2.64
Calcium oxide	3.42
Iron oxide	1.81
Magnesium oxide	0.28
LOI	4.9

3.2. Workability

The workability of FM mixes with different proportions of SDA as a substitute for cement; this is illustrated in Figure 9. We examined and compared the feasibility of the mixtures SDA10, SDA20, SDA30, SDA40, and SDA50 in comparison to the control mix, SDA0. As depicted in Figure 9, the integration of SDA resulted in a decrease in the workability of the FM. In comparison to the SDA0 mixture, it was observed that the workability values of all the evaluated SDA-blended FM mixtures exhibited a decrease. The SDA0 mixture demonstrated a measured slump flow value of 252 mm. The use of different proportions of SDA as a substitute for cement, specifically at levels of 10%, 20%, 30%, 40%, and 50%, resulted in equivalent decreases in workability of 1.19%, 1.98%, 2.38%, 2.38%, and 3.57%, respectively. The fast absorption of water leads to a reduction in the quantity of free water present in the FM mixture, thereby causing the solid particles to experience dissociation. This finding suggests that the workability of FM mixtures diminishes as the proportion of SDA increases, and that this condition becomes more pronounced with higher levels of cement replacement. A previous study on C25 concrete indicated a decrease in the workability of the mixtures when there was a partial replacement of cement with wood sawdust ash [40]. The decline in workability can be attributed to the hygroscopic nature of the substance, resulting in a fast uptake of moisture from the base mix [58]. In addition, the increased specific surface area of SDA requires a greater amount of water for the hydration process. The complex interaction of SDA particles also influences the workability of FM, resulting in enhanced cohesion and rigidity [59]. In the discipline of solid dynamics, the occurrence of heightened friction can be attributed to the irregular shape of the solid particles [60]. Also, it was noted that the air contents demonstrated an increase in correlation with higher proportions of SDA. The presence of holes and voids in the micrographs presented in Section 3.12 indicates high porosity, which is consistent with our expectations. Moreover, it is evident that the density of FM declines with the increase in the proportion of SDA. The observed reduction in density was mostly due to the lower specific gravity of SDA in comparison to cement and sand, as evidenced by the data presented in Table 1.

3.3. Consistency

Figure 10 shows the initial setting time and final setting time of FM mixes incorporating different proportions of SDA as a substitute for cement. We performed an assessment and comparison of the setting times of mixtures SDA10, SDA20, SDA30, SDA40, and SDA50, as well as the control mix SDA0. As depicted in Figure 10, the incorporation of SDA resulted in a noticeable increase in the setting times of the FM. In comparison to the SDA0 mixture, it was observed that the setting times of all of the evaluated SDA-blended FM mixtures exhibited an increase. The SDA0 mixture had initial and final setting times of 172 and 280 min, respectively. The replacement of cement with different proportions of SDA, specifically, 10%, 20%, 30%, 40%, and 50%, resulted in corresponding increases in the initial setting time of 6.78%, 9.30%, 12.79%, 15.70%, and 20.93%, respectively. Likewise, the final setting time increased by 3.57%, 6.43%, 9.64%, 11.79%, and 16.07%, correspondingly. The observed extension of both the initial and final setting times in the FM mixtures as the percentage of SDA increased indicates that the SDA materials reacted with water and prolonged the hydration response. The regular surface effects and decreased surface energy

displayed by SDA can be ascribed to this phenomenon [20]. The surface atoms exhibit a diminished level of activation and unreliability, resulting in a decreased reaction rate [61].

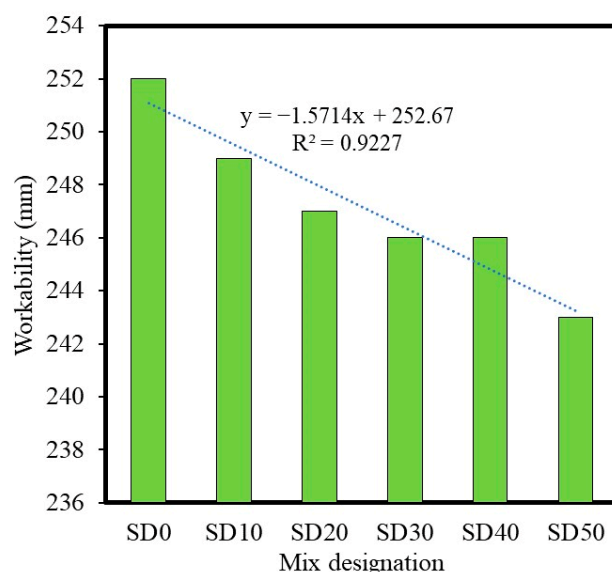


Figure 9. Workability of various FM mixes.

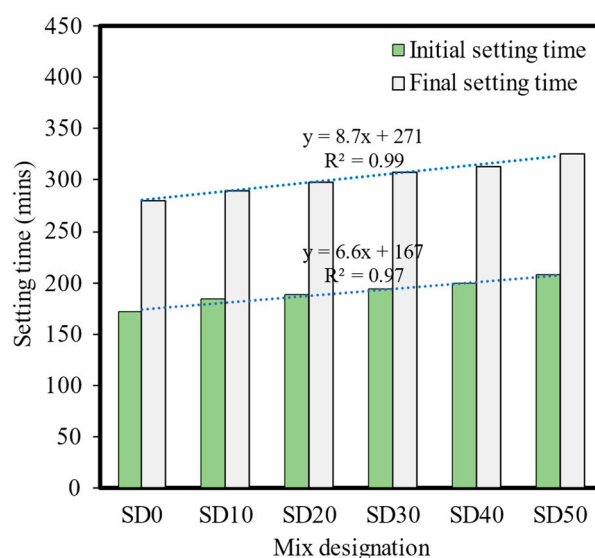


Figure 10. Initial and final setting times of various FM mixes.

3.4. Density

The wet, demolding, and dry densities of the FM depicted in Figure 11, highlighting the effects of different amounts of SDA used as a replacement for cement. The wet, demolding, and dry densities of the FM mixtures were determined and contrasted with the densities of the control FM mixture. The FM mixtures had different levels of cement replacement, with SDA contents ranging from 10% to 50%. When compared to the control FM mixture, all of the FM mixtures that used SDA as a replacement for cement exhibited reduced wet, demolding, and dry densities. When 10%, 20%, 30%, 40%, and 50% of the cement was replaced with SDA, the wet density of the FM decreased by 0.61%, 1.13%, 1.54%, 1.95%, and 2.56%, respectively. In a similar manner, the demolding and dry densities decreased by 0.67%, 1.22%, 1.87%, 2.33%, and 3.12%, respectively, and by 0.70%, 1.41%, 2.11%, 2.70%, and 3.28%, respectively. The decrease in the wet, demolding, and dry densities of FM when SDA is used as a partial replacement for cement may be due to the lower bulk density

of SDA compared to cement, as indicated in Table 2. The inclusion of SDA in the FM mix results in a reduction in its overall density, as sand particles possess a greater density compared to SDA [21]. As a result, the utilization of SDA as a replacement for cement results in reductions in the wet, demolding, and dry densities.

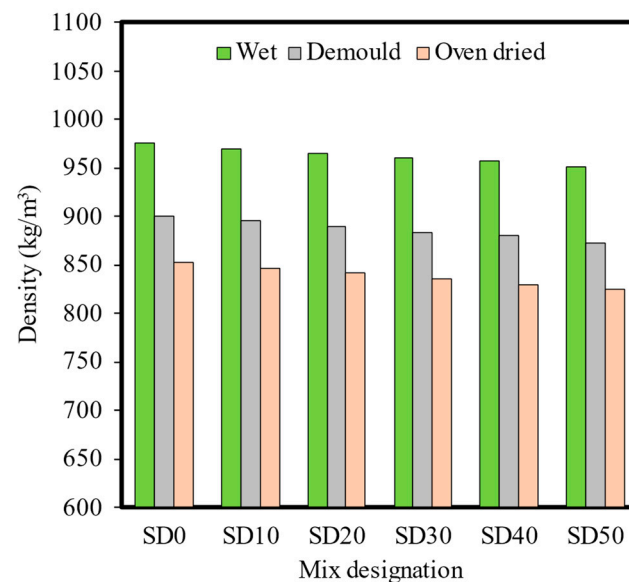


Figure 11. Wet, demolding, and oven-dried densities of various FM mixes.

3.5. Sorptivity

The findings of the sorptivity for the FM samples with varying levels of cement substitution (ranging from 0% to 50% SDA) are depicted in Figure 12. The increment of mass was then recorded at 10, 20, 30, 40, 50, and 60 min after the FM specimen was exposed to water. A graph of sorptivity (i , mm) was plotted against the square root of time (\sqrt{t}) at 7 and 28 days. Figure 12a,b shows that sorptivity experienced only a slight effect when the curing age was extended from 7 to 28 days. The formation of pores during the hydration process restricted the infiltration of water. The results of this study indicate that when including SDA as a substitute for cement, with a maximum replacement proportion of 20%, there was a significant reduction in the sorptivity of the FM specimens. The observed decreases in the water capillary absorption rates may be related to the action of surface tension in efficiently occupying the small pores and capillaries [22]. The sorptivity of the FM exhibited an increase when the replacement of cement with SDA exceeded 30%. This condition presumably arose because of an elevation in the typical transitory route of water in the FM specimens, which may be attributable to an increase in the number of trapped air voids resulting from the inappropriate inclusion of SDA in the cementitious composites. Consequently, the presence of entrained air gaps, also known as macropores, creates a more complex route for capillary flow relative to the foam volume [62]. This, in turn, mitigates the transport mechanism occurring within the matrix.

3.6. Porosity

Figure 13 illustrates the impact of varying percentages of cement replacement with SDA on the porosity of the FM. The FM samples were subjected to testing at four different ages of 7, 14, 28, and 90 days. The utilization of SDA in the manufacturing process of FM proved advantageous in mitigating the porosity rates across various mix compositions. Nevertheless, the utilization of 20% SDA as a cement replacement led to the lowest water absorption levels. This substitution led to decreases of approximately 5.71%, 5.78%, 6.27%, and 6.17% in water absorption compared to the control specimen at 7, 14, 28, and 90 days of age, respectively. This finding indicates that the utilization of SDA led to enhancements in both the pore distribution and pore connectivity, resulting in a decrease in the porosity

of the FM mixes. The observed phenomenon can be ascribed to the significant level of energy exhibited by SDA, resulting in the intake of a considerable quantity of hydration products [63]. As a result, the formation of a C-S-H gel occurred. Additionally, it is worth noting that the initial response of pozzolan takes place at the surface of the SDA, resulting in the development of durable C-S-H gel. The gel produced as a result ultimately leads to the creation of larger amounts of C-S-H gels. These gels efficiently fill the smaller pores within the specimen, hence contributing to the improvement of the pore structure and playing a significant part in reducing the porosity of the FM [64]. When the cement replacement with SDA exceeded 30%, there was an observed increase in the porosity of the FM. This condition presumably arose because of an escalation in the typical migration pathway of water in the FM samples, which can be attributed to a surge in trapped air voids resulting from the excessive integration of SDA.

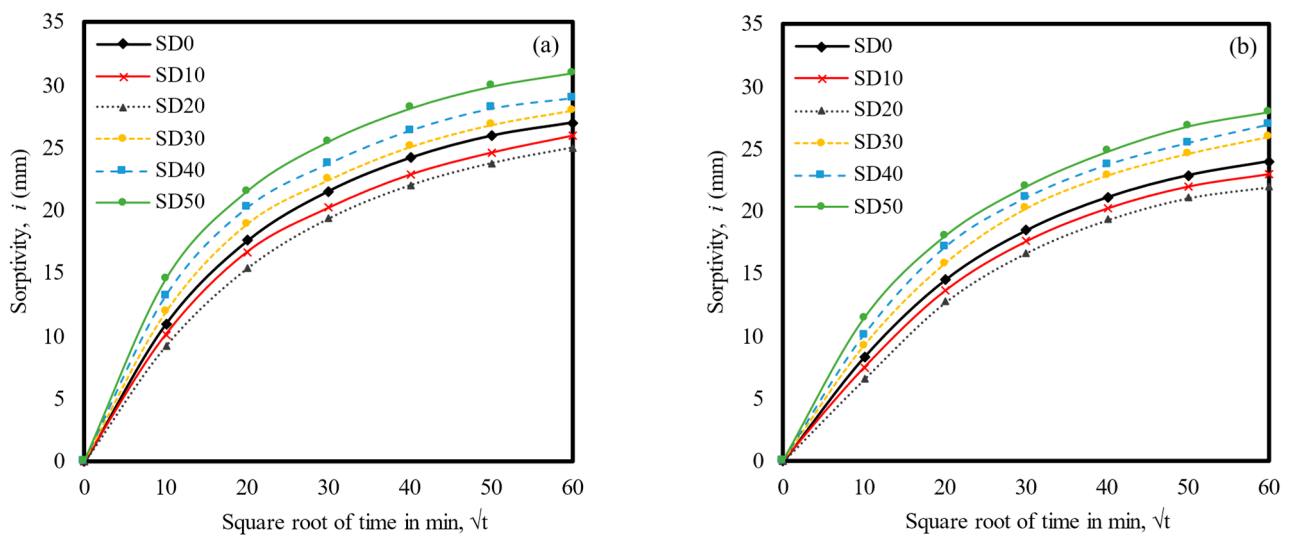


Figure 12. Sorptivity of various FM mixes: (a) day 7, (b) day 28.

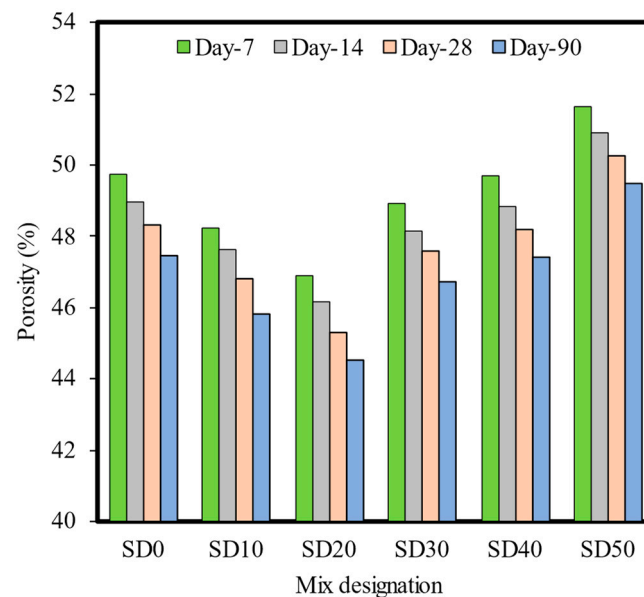


Figure 13. Porosity of various FM mixes.

3.7. Intrinsic Air Permeability

The intrinsic air permeability of FM is depicted in Figure 14, illustrating its relationship with the SDA percentage as a substitute for cement. The results indicate that the inclusion

of SDA led to an improvement in gas permeability, with a maximum improvement of 20% achieved when 20% of the cement was replaced. This resulted in a reduced gas permeability value of $0.374 \times 10^{-9} \text{ m}^2/\text{s}$. The observed progressive decrease indicates a reduction in pore size, interconnectivity, and more uniform distribution, hence restricting the flow of fluid via FM. There is a possibility of enhancing the microstructure inside the interfacial transition zones, which might result in a growth in the composition of the C-S-H gel. This, in turn, tends to cause a notable decrease in the intrinsic air permeability. These reactions result in an augmentation of the uniformity and robustness of the interfacial transition zones, accompanied by a reduction in their diameter [65]. An inverse relationship was seen as the cement replacement with SDA rose from 30% to 50%. Specifically, the intrinsic air permeability of the FM exhibited a modest rise of $0.447 \times 10^{-9} \text{ m}^2/\text{s}$, $0.478 \times 10^{-9} \text{ m}^2/\text{s}$, and $0.523 \times 10^{-9} \text{ m}^2/\text{s}$, respectively. The observed increase in intrinsic air permeability can be attributed to the greater utilization of SDA, which has a direct impact on the binder phase across the whole structure.

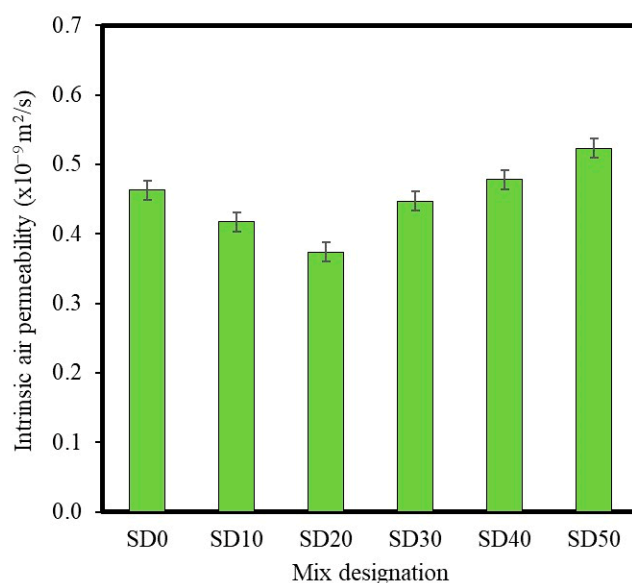


Figure 14. Intrinsic air permeability of various FM mixes.

3.8. Compressive Strength

According to the data shown in Figure 15, the compressive strength of the FM on day 7 with 10%, 20%, 30%, 40%, and 50% of the cement substituted with SDA was 1.36 MPa, 1.48 MPa, 1.05 MPa, 0.56 MPa, and 0.39 MPa, respectively. The compressive strength values on day 28 were 2.75 MPa, 2.95 MPa, 2.17 MPa, 1.78 MPa, and 1.42 MPa, respectively. The observed significant increase in the compressive strength of the FM blended with 20% SDA could be attributed to the increased intake of calcium hydroxide (CaOH)₂ formed during the cement hydration process [60]. Because of SDA's high flexibility, this observed behavior is most noticeable during the early stages of hydration. As a result, cement hydration occurs faster, resulting in the creation of more reaction products [14]. Furthermore, the formation of the extra stiffening gel has the potential to increase the restrictions associated with SDA distribution. The addition of SDA improves the particle packing density in FM, showing a reduction in the diameters of bigger pores in the cement paste [66]. After surpassing the optimal substitution of 20% cement with SDA, compressive strength began to drop. The observed occurrence can be attributed to the higher concentration of SDA in the mixture compared to the amount necessary to react with the lime released during the hydration phase. Although SDA was present in the cementitious matrix of the FM, it did not affect the strength of the composites.

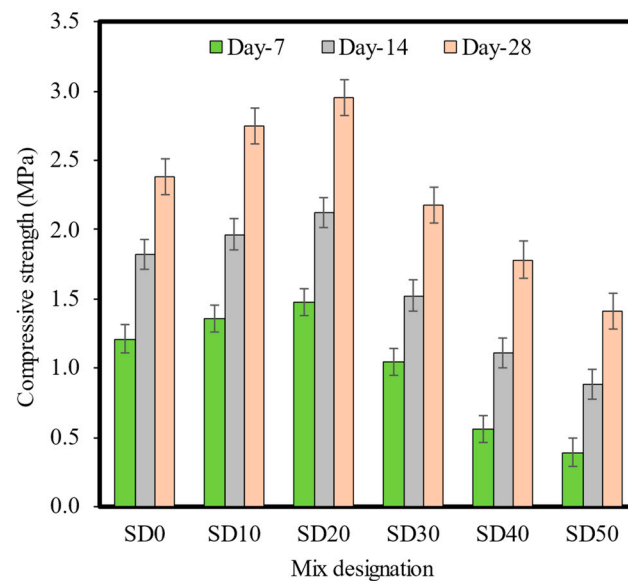


Figure 15. Compressive strength of various FM mixes.

3.9. Flexural Strength

The results of the flexural strength tests conducted on FM with the inclusion of SDA as a replacement for cement are depicted in Figure 16. The incorporation of SDA as a replacement for cement resulted in a significant improvement in the flexural strength of the FM. The investigation determined that the most beneficial substitution rate for cement with SDA was 20%, which signifies the optimal proportion for achieving the desired FM production. A substitution rate beyond 20% did not result in a favorable effect on the flexural strength. On the other hand, there was a decrease in flexural strength, which can be ascribed to the decrease in cement content. The flexural strengths of the FM samples after 28 days of testing were recorded as 0.61, 0.72, 0.80, 0.62, 0.48, and 0.38 MPa for the replacement rates of 0%, 10%, 20%, 30%, 40%, and 50%, respectively. The use of SDA has the potential to speed up the hydration of the tricalcium silicate (C3S) clinker phase. This behavior can be attributed to the SDA's highly sensitive surface area [54,55].

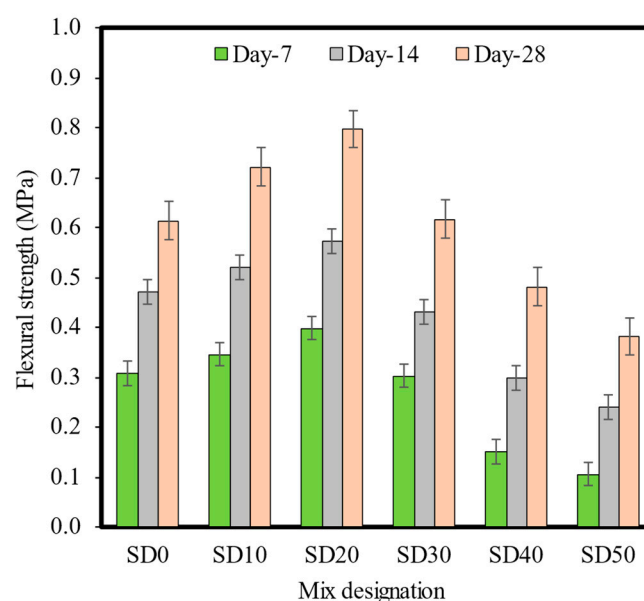


Figure 16. Flexural strength of various FM mixes.

3.10. Split Tensile Strength

Figure 17 shows the split tensile strength values for the control sample at 7, 14, and 28 days to be 0.20 MPa, 0.32 MPa, and 0.41 MPa, respectively. The split tensile strength of the FM was observed at three different ages (7, 14, and 28 days). The results indicated increases in the split tensile strength of 36.32%, 31.85%, and 33.33%, respectively, when 20% of the cement was replaced with SDA. Due to its substantial reactivity during the early stages of hydration, the addition of SDA plays a critical role in enhancing the FM's split tensile strength. Because of the considerable production of C-S-H gel within the matrix of the FM cementitious material, this phenomenon may be explained once more by the formation of the C-S-H gel in the cementitious matrix. By providing extra nucleation sites, SDA accelerates the process of hydration and promotes the formation of hydrated products in the early stages of hydration [67]. The findings of this study point to the potential use of SDA as a cement replacement in the 10% to 30% range to improve split tensile strength. The appropriate cement substitution rate in FM production was discovered to be 20% of the total cement used.

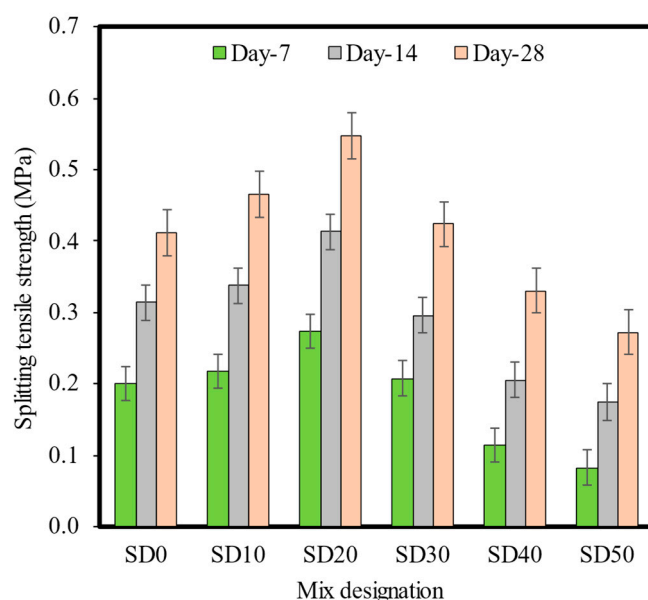


Figure 17. Splitting tensile strength of various FM mixes.

3.11. Thermal Conductivity

Figure 18 displays the thermal conductivity of FM with different proportions of SDA. The thermal conductivity of FM mixtures with varying concentrations of SDA (0%, 10%, 20%, 30%, 40%, and 50%) was measured and compared with the thermal conductivity of the control mixture. Overall, it was observed that the incorporation of SDA into FM led to a notable increase in the thermal conductivity of the FM when including 30% SDA content. The FM mixtures with SDA exhibited higher thermal conductivity values as compared to the control FM mixture. The thermal conductivity of the control FM mixture was quantified and recorded at 0.271 W/mK. The thermal conductivity demonstrated increases of 2.21%, 4.80%, and 2.58% when incorporating 10%, 20%, and 30% SDA, respectively. When the addition of SDA reached 40% and 50%, the thermal conductivity values experienced improvements of 0.74% and 2.58%, respectively. The incorporation of SDA into the FM led to significant increases in thermal conductivity, suggesting a change in the pore structure. The observed phenomena can be ascribed to the reduced pore size in FC specimens with SDA in comparison to the control FC specimen. In contrast, the diameters of the pores exhibited an increase when the replacement of cement with SDA reached 40%. The microstructural analysis of the FM samples containing 40% and 50% SDA revealed higher levels of porosity, characterized by a greater prevalence of irregular forms. This phenomenon can be

attributed to the influence of dispersion on the cement, resulting in a morphology that exhibited reduced compaction and increased porosity in its natural state [67].

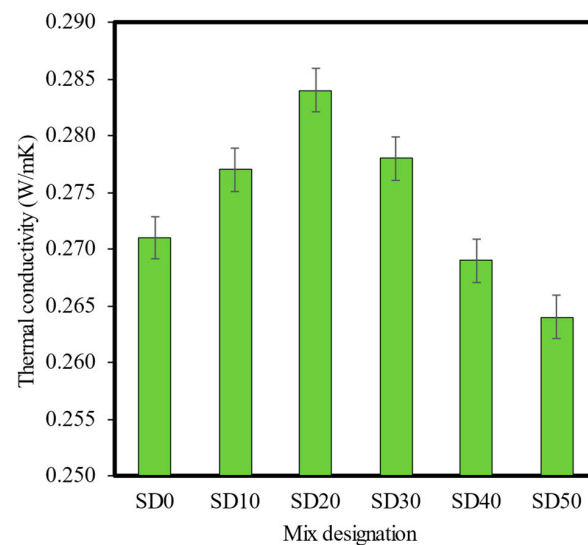


Figure 18. Thermal conductivity of various FM mixes.

3.12. Physical Characterization

The results shown in Figure 19 clearly demonstrate that an increased proportion of SDA resulted in a consistent decrease in the volume of pores larger than 200 μm in the specimens. This trend persisted until the ideal SDA percentage of 20%. This observation indicates an increase in the packing density of the FM material and an enhancement in the structure of its pores. The integration of SDA into the compositions resulted in a reduction in the overall porosity. Our findings further demonstrated that the utilization of an FM mixture with 20% SDA exhibited the greatest proportion of pore widths measuring below 100 μm . These observations can be attributed to the interference of capillary holes resulting from the intensified creation of C–S–H gel [68]. Conversely, when the SDA percentage was increased beyond 30%, there was a corresponding increase in the fraction of pores exceeding 200 μm in size. The reported outcomes may be attributed to the dispersion of the cement, which resulted in the breakdown of the FM matrix. The phenomenon of degradation likely played a role in the development of both larger and irregularly shaped pores.

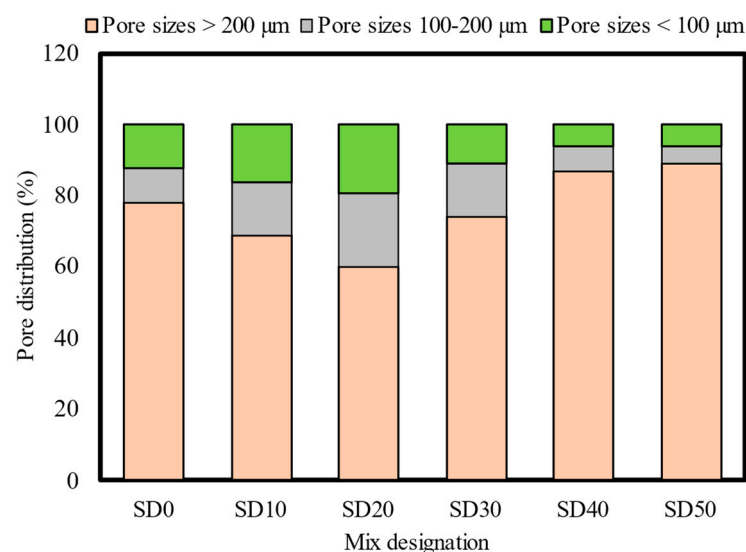


Figure 19. Pore distributions of various FM mixes.

The scanning electron microscope (SEM) images of the FM mixes with different amounts of SDA as a substitute for cement are shown in Figure 20. The SEM images show that the addition of varying quantities of SDA to the FM, from 0% (control) to 50%, significantly affected the pore structure of the FM. The control sample's SEM examination, as shown in Figure 20a, showed an irregular pattern of pores with notable fluctuations in size and irregularity. The microstructure of the FM mixes containing 10% and 20% SDA showed a considerably denser structure (as indicated in Figure 20b,c), and smaller voids were seen when compared to the control FM specimen. The observed sample showed a more homogeneous and densely uniform structure in comparison to the control sample. As seen in Figure 20a, the control FM specimens showed a mild adhesion between the paste and sand. On the other hand, as shown in Figure 20c, the FM specimen with 20% SDA showed outstanding sand–paste adhesion. Conversely, as Figure 20d–f illustrates, there was a discernible increase in the pore diameter when the SDA content surpassed 30%. The FM sample with 50% SDA showed greater porosity when examined microstructurally. This porosity was mainly seen in irregular shapes, as illustrated in Figure 20f. The presence of increased amounts of SDA beyond the ideal percentage resulted in the dispersion of voids and interface gaps within the FM microstructure. Mixtures containing higher proportions of SDA exhibited a greater number and larger size of voids. These findings were supported by the results of the mechanical properties tests performed as part of this investigation. These data show that using more than 30% SDA reduces the strength properties as compared to FM specimens with 20% SDA.

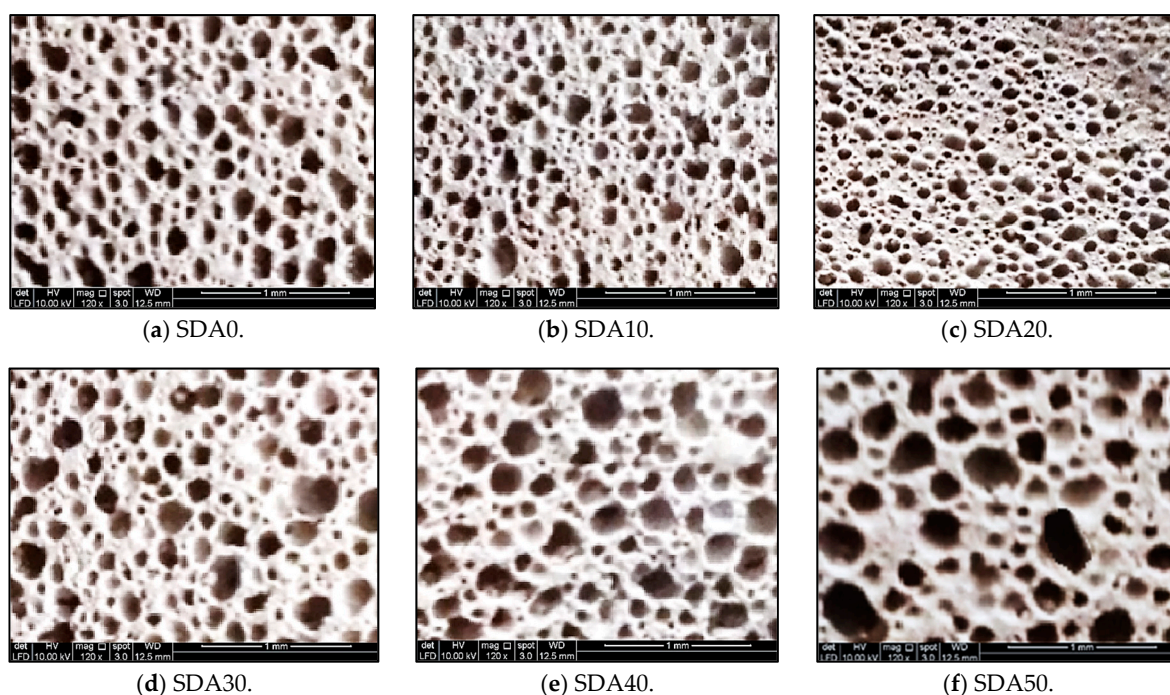


Figure 20. SEM images of various FM mixes.

4. Conclusions

The aim of this study was to examine the various properties of foamed mortar (FM) with different percentages of sawdust ash (SDA) used as a substitute for cement. The properties evaluated included the fresh-state, mechanical, thermal, microstructural, and transport properties. The study included six distinct SDA cement replacement levels, namely, 0% (serving as the control sample), 10%, 20%, 30%, 40%, and 50%. With regard to the findings from the experiments of this study, the following conclusions can be drawn:

1. The workability of FM is reduced by the introduction of SDA at higher percentages. When compared to the SDA0 mix, the slump readings for the SDA50 mix decreased by about 3.19%. Additionally, it was discovered that the density of the FM mixtures was directly related to the percentage of SDA substitution, which might be explained by the fact that SDA has a different specific gravity and density to OPC.
2. The transport properties of the FM–SDA composites, including porosity, intrinsic air permeability, and sorptivity, exhibited a linear improvement as the proportion of SDA increased, up to 20%. Once the cement replacement by SDA exceeded 30%, there was a noticeable degradation in these properties.
3. The mechanical strength properties of FM significantly improved when SDA was used to replacing up to 20% of the cement, but they deteriorated when the replacement rate was more than 30%.
4. Large and merging voids appeared in the FM's cementitious matrix when the addition of SDA exceeded 30% cement replacement. According to SEM analysis, those FM blends with higher SDA contents had voids that were more apparent and larger.
5. Based on the findings of this study, it is recommended to incorporate a cement replacement range of 10–20% with sawdust in the production process of FM to achieve favorable mechanical, thermal, and transport properties.
6. The findings of this study demonstrate the potential for adopting SDA as a substitute for cement in the production of FM. Further research is warranted to explore the chemical composition and long-term durability characteristics of hydration products in SDA–FM composites, as well as to conduct EDS analysis on fractured SDA–FM specimens.

Funding: Open access funding provided by Nawroz University Centre for Scientific Research and Development. This work was conducted without external funding.

Institutional Review Board Statement: Not applicable.

Informed Consent Statement: Not applicable.

Data Availability Statement: Data are contained within the article.

Conflicts of Interest: The author declared no potential conflicts of interest with respect to the research, authorship, and/or publication of this article.

References

1. Serri, E.; Suleiman, M.Z. The influence of mix design on mechanical properties of oil palm shell lightweight concrete. *J. Mater. Environ. Sci.* **2015**, *6*, 607–612.
2. Musa, M.; Abdul Ghani, A.N. Influence of oil palm empty fruit bunch (EFB) fibre on drying shrinkage in restrained lightweight foamed mortar. *Int. J. Innov. Technol. Exp. Eng.* **2019**, *8*, 4533–4538. [\[CrossRef\]](#)
3. Maglad, A.M.; Dip Datta, S.; Tayeh, B.A. Assessing the mechanical, durability, thermal and microstructural properties of seashell ash based lightweight foamed concrete. *Constr. Build Mater.* **2023**, *402*, 133018. [\[CrossRef\]](#)
4. Ganesan, S.; Che, A.A.I.; Sani, N. Performance of polymer modified mortar with different dosages of polymeric modifier. *MATEC Web Conf.* **2014**, *15*, 01039. [\[CrossRef\]](#)
5. Mydin, M.A.O. Thin-walled steel enclosed lightweight foamcrete: A novel approach to fabricate sandwich composite. *Australian J. Basic Appl. Sci.* **2011**, *5*, 1727–1733.
6. Tambichik, M.A.; Abdul Samad, A.A.; Mohamad, N.; Mohd Ali, A.Z.; Mohd Bosro, M.Z.; Iman, M.A. Effect of combining Palm Oil Fuel Ash (POFA) and Rice Husk Ash (RHA) as partial cement replacement to the compressive strength of concrete. *Int. J. Integr. Eng.* **2018**, *10*, 61–67. [\[CrossRef\]](#)
7. Nensok, M.H.; Awang, H. Fresh state and mechanical properties of ultra-lightweight foamed concrete incorporating alkali treated banana fibre. *J. Teknol.* **2022**, *84*, 117–128. [\[CrossRef\]](#)
8. Awang, H.; Roslan, A.F. Effects of fibre on drying shrinkage, compressive and flexural strength of lightweight foamed concrete. *Adv. Mater. Res.* **2012**, *587*, 144–149.
9. Nensok, M.H.; Awang, H. Investigation of Thermal, Mechanical and Transport Properties of Ultra Lightweight Foamed Concrete (UFC) Strengthened with Alkali Treated Banana Fibre. *J. Adv. Res. Fluid Mech. Therm. Sci.* **2021**, *86*, 123–139. [\[CrossRef\]](#)
10. Nawi, M.N.M.; Osman, W.N.; Rofie, M.K.; Lee, A. Supply chain management (SCM): Disintegration team factors in Malaysian Industrialised Building System (IBS) construction projects. *Int. J. Supply Chain Manag.* **2018**, *7*, 140–143.
11. Sany, N.M.; Taib, M.; Mohd Alias, N. Imperative causes of delays in construction projects from developers' outlook. *MATEC Web Conf.* **2014**, *10*, 06005.

12. Esruq-Labin, A.M.J.; Che-Ani, A.I.; Tawil, N.M.; Nawi, M.N.M. Criteria for Affordable Housing Performance Measurement: A Review. *E3S Web Conf.* **2014**, *3*, 01003. [\[CrossRef\]](#)
13. Suhaili, S.S.; Othuman Mydin, M.A.; Awang, H. Influence of Mesocarp Fibre Inclusion on Thermal Properties of Foamed Concrete. *J. Adv. Res. Fluid Mech. Therm. Sci.* **2021**, *87*, 1–11. [\[CrossRef\]](#)
14. Serudin, A.M.; Ghani, A.N.A. Effect of lightweight foamed concrete confinement with woven fiberglass mesh on its drying shrinkage. *Rev. Ing. Constr.* **2021**, *36*, 21–28. [\[CrossRef\]](#)
15. Suhaili, S.S.; Othuman Mydin, M.A. Potential of stalk and spikelets of empty fruit bunch fibres on mechanical properties of lightweight foamed concrete. *Int. J. Sci. Technol. Res.* **2020**, *9*, 3199–3204.
16. Phius, A.F.; Sani, N.M.; Tawil, N.M. Potential of Green Construction in Malaysia: Industrialised Building System (IBS) vs. Traditional Construction Method. *E3S Web Conf.* **2014**, *3*, 01009.
17. Mohamed Shajahan, M.F.; Ganesan, S.; Sani, N.M. Laboratory investigation on compressive strength and micro-structural features of foamed concrete with addition of wood ash and silica fume as a cement replacement. *MATEC Web Conf.* **2014**, *17*, 01004.
18. Zamzani, N.M.; Abdul Ghani, A.N. Experimental data on compressive and flexural strengths of coir fibre reinforced foamed concrete at elevated temperatures. *Data Brief.* **2019**, *25*, 104320.
19. Zamzani, N.M.; Ghani, A.N.A. Effectiveness of ‘cocos nucifera linn’ fibre reinforcement on the drying shrinkage of lightweight foamed concrete. *ARN J. Eng. Appl. Sci.* **2019**, *14*, 3932–3937.
20. Maglad, A.M.; Othuman Mydin, M.A.; Majeed, S.S.; Tayeh, B.A.; Mostafa, S.A. Development of eco-friendly foamed concrete with waste glass sheet powder for mechanical, thermal, and durability properties enhancement. *J. Build. Eng.* **2023**, *80*, 107974. [\[CrossRef\]](#)
21. Alyami, M.; Mydin, M.A.O.; Zeyad, A.M.; Majeed, S.S.; Tayeh, B.A. Influence of wastepaper sludge ash as partial cement replacement on the properties of lightweight foamed concrete. *J. Build. Eng.* **2023**, *79*, 107893. [\[CrossRef\]](#)
22. Mydin, M.A.O.; Hamah Sor, N.; Althoei, F.; Deifalla, A.F.; Tawfik, T.A. Performance of lightweight foamed concrete partially replacing cement with industrial and agricultural wastes: Microstructure characteristics, thermal conductivity, and hardened properties. *Ain Shams Eng. J.* **2023**, *14*, 102546. [\[CrossRef\]](#)
23. Behera, M.; Bhattacharyya, S.K.; Minocha, A.K.; Deoliya, R.; Maiti, S. Recycled aggregate from C&D waste & its use in concrete—A breakthrough towards sustainability in construction sector: A review. *Constr. Build. Mater.* **2014**, *68*, 501–516.
24. Nambiar, E.; Ramamurthy, K. Air-void characterisation of foam concrete. *Cem. Concr. Res.* **2007**, *37*, 221–230. [\[CrossRef\]](#)
25. Ramamurthy, K.; Kunhanandan Nambiar, E.K.; Indu Siva Ranjani, G. A classification of studies on properties of foam concrete. *Cem. Concr. Compos.* **2009**, *31*, 388–396. [\[CrossRef\]](#)
26. Kearsley, E. The Effect of High Volume of Ungraded Fly Ash on the Properties of Foamed Concrete. Ph.D. Thesis, School of Civil Engineering, The University of Leeds, Leeds, UK, 1999.
27. Jalal, M.; Tanveer, A.; Jagdeesh, K.; Ahmed, F. Foam concrete. *Int. J. Civ. Eng. Res.* **2017**, *8*, 2278–3652.
28. Kearsley, E.P.; Wainwright, P.J. The effect of high fly ash content on the compressive strength of foamed concrete. *Cem. Concr. Res.* **2001**, *31*, 105–112. [\[CrossRef\]](#)
29. Mydin, M.A.O.; Nawi, M.N.M.; Odeh, R.A.; Salameh, A.A. Durability Properties of Lightweight Foamed Concrete Reinforced with Lignocellulosic Fibers. *Materials* **2022**, *15*, 4259. [\[CrossRef\]](#)
30. Mohd Nawi, M.N.; Mohamed, O.; Sari, M.W. Mechanical Properties of Lightweight Foamed Concrete Modified with Magnetite (Fe₃O₄) Nanoparticles. *Materials* **2022**, *15*, 5911.
31. Cai, J.; Pan, G.; Li, E.M. Behaviors of eccentrically loaded ECC-encased CFST columns after fire exposure. *Eng. Struct.* **2023**, *289*, 116258. [\[CrossRef\]](#)
32. Ghanim, A.A.J.; Amin, M.; Zeyad, A.M.; Tayeh, B.A.; Agwa, I.S.; Elsakhawy, Y. Effect of polypropylene and glass fiber on properties of lightweight concrete exposed to high temperature. *Adv. Concr. Construct.* **2023**, *15*, 179–190.
33. Olaiya, B.C.; Lawan, M.M.; Olonade, K.A. Utilization of sawdust composites in construction—A review. *SN Appl. Sci.* **2023**, *5*, 140. [\[CrossRef\]](#)
34. Aigbomian, E.P.; Fan, M. Development of wood-crete from treated sawdust. *Constr. Build. Mater.* **2014**, *52*, 353–360. [\[CrossRef\]](#)
35. Cheah, C.B.; Ramli, M. The engineering properties of high-performance concrete with HCWA-DSF supplementary binder. *Constr. Build. Mater.* **2013**, *40*, 93–103. [\[CrossRef\]](#)
36. Okoro, N.J.M.; Ozonoh, M.; Harding, K.G.; Oboirien, B.O.; Daramola, M.O. Potentials of torrefied pine sawdust as a renewable source of fuel for pyro-gasification: Nigerian and South African perspective. *ACS Omega* **2021**, *6*, 3508–3516. [\[CrossRef\]](#) [\[PubMed\]](#)
37. Zou, S.; Li, H.; Wang, S.; Jiang, R.; Zou, J.; Zhang, X.; Liu, L.; Zhang, G. Experimental research on an innovative sawdust biomass-based insulation material for buildings. *J. Clean. Prod.* **2020**, *260*, 121029. [\[CrossRef\]](#)
38. Sajjad, A.M.; Norwati, J.; Wan Ibrahim, M.H.; Noridah, M.; Samiullah, S. Utilization of Sawdust Ash as Cement Replacement for the Concrete Production: A Review. *Eng. Sci. Technol. Int. Res. J.* **2017**, *1*, 11–15.
39. Abdullahi, A.; Abubakar, M.; Afolayan, A. Partial Replacement of Sand with Sawdust in Concrete Production. In Proceedings of the 3rd Biennial Engineering Conference, Federal University of Technology, Minna, Nigeria, 14–16 May 2013.
40. Bikila, M.; Joshua, O.I. Utilization of Cordia Africana wood sawdust ash as partial cement replacement in C 25 concrete. *Clean. Mater.* **2021**, *1*, 100012.
41. Narayanan, A.; Hemnath, G.; Sampaul, K.; Mary, A. Replacement of Fine Aggregate with Sawdust. *Int. J. Adv. Res. Basic Eng. Sci. Technol.* **2017**, *3*, 206–210.

42. Velmurugan, P.J.; Jose, R.B. Effect on Strength Properties of M30 Grade of Concrete by Using Waste Wood Powder as Partial Re-placement of Sand. *Int. J. Eng. Manag. Res.* **2017**, *7*, 301–305.
43. *BS EN 197-1*; Cement—Composition, Specifications, and Conformity Criteria for Common Cement. British Standards Institute: London, UK, 2011.
44. *ASTM C33-03*; Standard Specification for Concrete Aggregates. American Society for Testing and Materials. ASTM International: West Conshohocken, PA, USA, 2003.
45. *BS EN 3148*; Water for Making Concrete (Including Notes on the Suitability of the Water). British Standards Institute: London, UK, 1980.
46. *ASTM C 230-97*; Flow Table for Use in Tests of Hydraulic Cement. American Society for Testing and Materials. ASTM International: West Conshohocken, PA, USA, 1997.
47. *B.E. 196-3*; British Standard Methods of Testing Cement—Part 3: Determination of Setting Times and Soundness. Br. Stand. British Standards Institute: London, UK, 2003.
48. *BS 12350-6*; Testing Fresh Concrete—Part 6: Density. Czech Office for Standards; Metrology and Testing: Prague, Czech Republic, 2020.
49. Cabrera, J.G.; Lynsdale, C.J. A new gas permeameter for measuring the permeability of mortar and concrete. *Mag. Concr. Res.* **1988**, *40*, 177–182. [[CrossRef](#)]
50. *ASTM C 1403*; Standard Test Method for Rate of Water Absorption of Masonry Mortars. ASTM International: West Conshohocken, PA, USA, 2005.
51. *British Standard BS 1881-122*; Testing Concrete, Method for Determination of Water Absorption. British Standards Institute: London, UK, 1983.
52. *BS EN 12390-3*; Testing Hardened Concrete: Compressive Strength of Test Specimens. British Standards Institute: London, UK, 2019; pp. 1–15.
53. *BS EN 12390-Part 5*; Testing Hardened Concrete Part 5: Flexural Strength of Test Specimens. British Standards Institute: London, UK, 2019.
54. *BS EN 12390-6*; Testing Hardened Concrete—Part 6: Tensile Splitting Strength of Test Specimens. British Standards Institute: London, UK, 2010; pp. 1–15.
55. *ASTM, C469, C469M-14*; Standard Test Method for Static Modulus of Elasticity and Poisson's Ratio of Concrete in Compression. ASTM International: West Conshohocken, PA, USA, 2014.
56. *ASTM C177*; Test Method for Steady-State Thermal Transmission Properties by Means of the Guarded Hot Plate. Latest Revision; ASTM International: West Conshohocken, PA, USA, 1990.
57. *ASTM D4404-18*; Standard Test Method for Water Retention Curve of Determination of Pore Volume and Pore Volume Distribution of Soil and Rock by Mercury Intrusion Porosimetry. ASTM International: West Conshohocken, PA, USA, 2018.
58. Cheng, Y.; You, W.; Zhang, C.; Li, H.; Hu, J. The implementation of waste sawdust in concrete. *Engineering* **2013**, *5*, 943–947. [[CrossRef](#)]
59. Siddique, R.; Singh, M.; Singhal, A. Use of unprocessed wood ash as partial replacement of sand in concrete. *ACI Mater. J.* **2019**, *116*, 77–86. [[CrossRef](#)]
60. Chowdhury, S.; Maniar, A.; Suganya, O. Strength development in concrete with wood ash blended cement and use of soft computing models to predict strength parameters. *J. Adv. Res.* **2015**, *6*, 907–913. [[CrossRef](#)]
61. Charis, G.; Danha, G.; Muzenda, E. A review of timber waste utilization: Challenges and opportunities in Zimbabwe. *Procedia Manuf.* **2019**, *35*, 419–429. [[CrossRef](#)]
62. Bouguerra, A.; Amiri, O.; Ait-Mokhtar, A.; Diop, M.B. Water sorptivity and pore structure of wood cementitious composites. *Mag. Concr. Res.* **2002**, *54*, 103–112. [[CrossRef](#)]
63. Corinaldesi, V.; Mazzoli, A.; Siddique, R. Characterization of lightweight mortars containing wood processing by-products waste. *Construct. Build. Mater.* **2016**, *123*, 281–289. [[CrossRef](#)]
64. Vaickelionis, G.; Vaickelionene, R. Cement hydration in the presence of wood extractives and pozzolan mineral additives. *Ceramics* **2006**, *50*, 115–122.
65. El-Nadoury, W. Production of Sustainable Concrete using Sawdust. *Mag. Civ. Eng.* **2021**, *105*, 10507.
66. Osei, D.Y.; Jackson, E.N. Compressive Strength of Concrete Using Sawdust as Aggregate. *Int. J. Sci. Eng. Res.* **2016**, *7*, 1349–1353.
67. Sales, A.; de Souza, F.; dos Santos, W.; Zimer, A.; do Couto Rosa Almeida, F. Lightweight composite concrete produced with water treatment sludge and sawdust: Thermal properties and potential application. *Construct. Build. Mater.* **2010**, *24*, 2446–2453. [[CrossRef](#)]
68. Awal, A.A.; Mariyana, A.; Hossain, M. Some Aspects of Physical and Mechanical Properties of Sawdust Concrete. *Int. J. Geomate* **2016**, *10*, 1918–1923.

Disclaimer/Publisher's Note: The statements, opinions and data contained in all publications are solely those of the individual author(s) and contributor(s) and not of MDPI and/or the editor(s). MDPI and/or the editor(s) disclaim responsibility for any injury to people or property resulting from any ideas, methods, instructions or products referred to in the content.